 DOI: 10.1086/677544

Appendix B from A. B. Ryabov and B. Blasius, "Depth of the Biomass Maximum Affects the Rules of Resource Competition in a Water Column"

(Am. Nat., vol. 184, no. 5, p. E132)

Supplementary Information

Numerical Calculation of the IT and Its Slope γ

To obtain an IT numerically, we first calculate the equilibrium distribution of the resident species and then successively simulate the growth of a large ensemble of potential invaders with different half-saturation constants in the presence of the resident. Finally, using equation (5), we identify the combination of critical resource values that yield zero net growth for the invading species.

To find the slope of invasion thresholds, γ, numerically, we first calculate the equilibrium solution of the resident species and then successively simulate the growth of an ensemble of invaders with the following resource requirements:

$$\log(N^*_{\text{inv}}) = R_0 \cos\tilde{\gamma} + \log(N^*_{\text{res}}),$$

$$\log(I^*_{\text{inv}}) = -R_0 \sin\tilde{\gamma} + \log(I^*_{\text{res}}),$$

where the parameter $\tilde{\gamma}$ varies from 0 to 2π. This one parametric family describes invaders with critical resources placed along a circle of radius R_0 centered at the point $(N^*_{\text{res}}, I^*_{\text{res}})$ in the resource plane with a log-log scale. For simulations we used $R_0 = 0.3$; therefore, the maximal difference between the invader's and residents' critical resource requirements is $10^{0.3} \approx 2$.

Next, to obtain the slope of the invasion threshold, we use the bisection method for finding roots of the equation

$$G(\tilde{\gamma}) = 0,$$

where G is the total net growth rate of an invader in the presence of the resident. This equation has two solutions, γ^{N} and γ^{I}, which correspond to the invaders with lower nutrient and lower light requirements, respectively. For the final result, we calculate the average slope as

$$\gamma = \frac{(\gamma^{\text{N}} - \pi) + \gamma^{\text{I}}}{2}.$$

Logarithmic Resource Gradients

The shape and slope of the IT depend on the resource distributions. Ryabov and Blasius (2011) showed that if phytoplankton growth peaks in the deep layers of a water column, then the IT can be approximated by a straight line on a double-logarithmic scale (gray line in fig. 1*c*) with slope

$$\gamma_i \approx \frac{c_{\text{I},i}}{c_{\text{N},i}}. \tag{B1}$$

Here,

$$c_{\text{N},i} = \frac{1}{N}\frac{dN(z)}{dz}\bigg|_{\text{Sp}\,i}, \qquad c_{\text{I},i} = -\frac{1}{I}\frac{dI(z)}{dz}\bigg|_{\text{Sp}\,i} \tag{B2}$$

are the logarithmic resource gradients in equilibrium within the production layer that are shaped by the resident species, Sp *i*, in monoculture. This formula is exact if the resource distributions depend exponentially on depth z (as is typically

the case within the production layer); otherwise, it is valid for invaders with resource requirements that are sufficiently close to those of the resident. Thus, in this approximation the invasion threshold is parallel to (but does not, in general, coincide with) the curve $(N(z), I(z))$ in the resource plane parameterized by depth (Ryabov et al. 2010; Ryabov and Blasius 2011).

Here we analytically derive the relation between the density of the biomass of the resident and the resource gradients shaped by this species in equilibrium. First, we make use of the fact that the small spatial variation of the phytoplankton density within the production allows an approximation by a rectangular distribution. That is, we assume that the biomass has nonvanishing density $\overline{P}$ only within a layer of width w, where $\overline{P}$ is the average density within the production layer and $w = \int P(z)dz/\overline{P}$. Then, according to equation (4), the absolute value of the logarithmic gradient of light intensity is constant and equals

$$c_{\mathrm{I}} = -\frac{d\ln I(z)}{dz} = K_{\mathrm{bg}} + k\overline{P}, \tag{B3}$$

and the light distribution can be written as

$$\tilde{I}(z) = I^{*}e^{-c_{\mathrm{I}}(z-z_{\mathrm{I}})}, \tag{B4}$$

where z_{I} is the depth at which production of the resident becomes light limited (the lower boundary of the production layer).

To find the nutrient distribution, we assume that in the range of depths where the nutrient limits phytoplankton growth, the resources are depleted to low levels, at which a linear dependence gives a good approximation of the Monod kinetics. Thus, the linearized growth rate can be represented as $\mu(N) \approx \mu_{\max}N/H_{\mathrm{N}}$. Substituting this expression into equation (3), we obtain, in equilibrium,

$$-\alpha\mu_{\max}\frac{N}{H_{\mathrm{N}}}\overline{P} + D\frac{dN}{dz^{2}} = 0.$$

A solution to this equation that monotonically increases with depth gives the equilibrium nutrient distribution in the vicinity of the depth of nutrient limitation, z_{N},

$$\tilde{N}(z) = N^{*}e^{c_{\mathrm{N},\mathrm{I}}(z-z_{\mathrm{N}})}, \tag{B5}$$

with the logarithmic gradient

$$c_{\mathrm{N}} = \frac{d\ln N(z)}{dz} = \sqrt{\frac{\alpha\mu_{\max}\overline{P}}{DH_{\mathrm{N}}}}. \tag{B6}$$

Calculating the ratio of resource gradients, we obtain the slope of the IT,

$$\gamma = \frac{c_{\mathrm{I}}}{c_{\mathrm{N}}} = \sqrt{\frac{DH_{\mathrm{N}}}{\alpha\mu_{\max}}}\left(\frac{K_{\mathrm{bg}}}{\sqrt{\overline{P}}} + k\sqrt{\overline{P}}\right). \tag{B7}$$

This function decreases with $\overline{P}$ for $k\overline{P} < K_{\mathrm{bg}}$, reaches its minimum at $k\overline{P} = K_{\mathrm{bg}}$, and starts to increase when $k\overline{P} > K_{\mathrm{bg}}$. Since the resident biomass density increases with the nutrient supply (Beckmann and Hense 2007), increasing N_{B} will favor low-light-adapted invaders if $k\overline{P} < K_{\mathrm{bg}}$ and low-nutrient-adapted invaders as phytoplankton light attenuation becomes greater than background turbidity.

Potential Transitions in Species Composition

The diagrams in figure B1 represent the variety of potential transitions in species composition with increasing N_{B}. In these diagrams, the insets along the vertical and horizontal axes schematically show the effect of N_{B} on the slope of the IT, and the inner cells represent the corresponding outcomes of competition. If the dependences $\gamma_{1,2}(N_{\mathrm{B}})$ intersect the critical level only once (as in fig. 4*a*), then the diagram has only two columns and two rows, which correspond to four different outcomes (fig. B1*a*). Similar to uniform systems, we observe either coexistence or bistability at intermediate values of resource availability.

If, however, $\gamma_{1,2}(N_{\mathrm{B}})$ intersect the critical level more than once, the different ranges should be included as rows or columns of such diagram. For the situation shown in figure 4*b*, for every competitor we have two intervals where $\gamma_i > \gamma^{*}$ and two intervals where $\gamma_i < \gamma^{*}$. Consequently, every axis in figure B1*b* contains four insets, which leads to a total of

16 inner cells. This gives rise to a large variety of possible transitions in species composition. Two exemplary scenarios are indicated by the gray and green arrows. In general, in such a checkerboard-like diagram we can observe transitions between all possible outcomes of competition for the same two competitors.

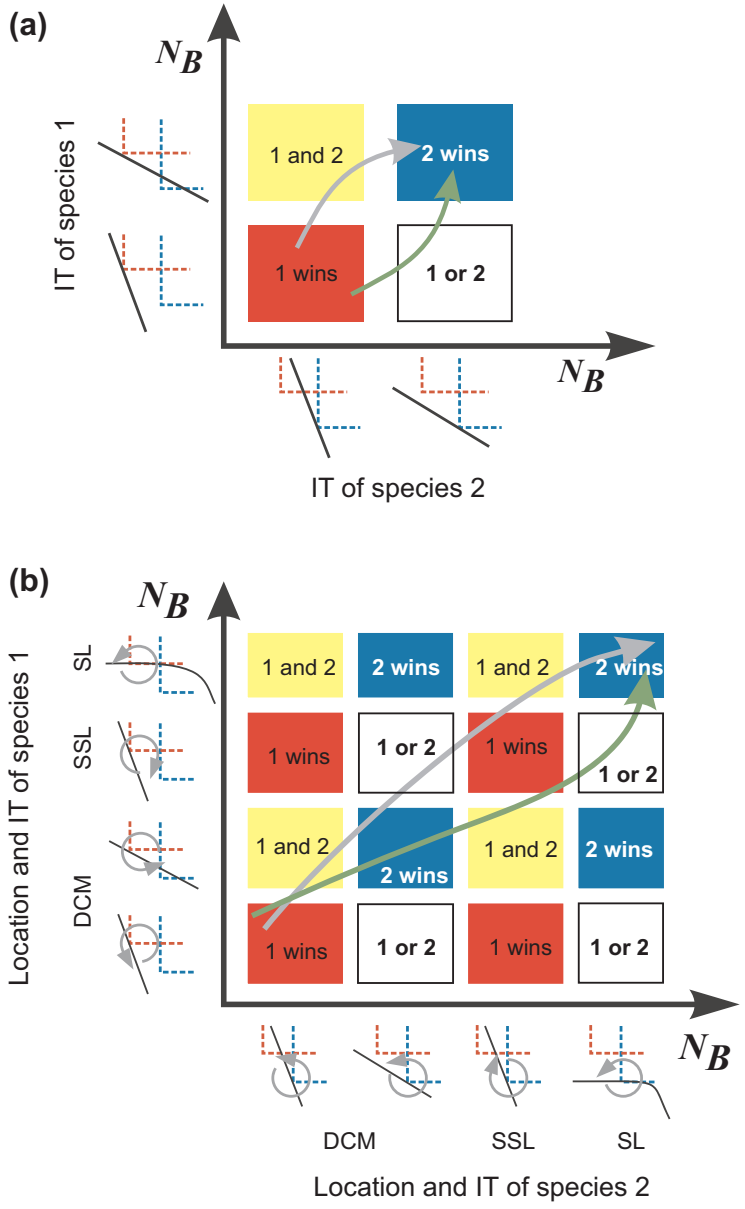

Figure B1: Potential transitions in species composition. Diagrammatic representation of all possible competition outcomes (inner cells) and sketch of the invasion thresholds (ITs) in the resource plane (insets along the axes). *a*, Simple scenario when the curves $\gamma(N_B)$ intersect the critical level γ^* only once (as in fig. 4*a*). The arrows sketch the only two possible transitions in species composition with increasing N_B. *b*, Multiple intersections of $\gamma_{1,2}(N_B)$ with the critical level γ^* (as in fig. 4*b*) lead to multiple transitions in the species composition. The gray and green arrows show two of the many possible transitions and correspond to the transitions shown by the gray arrows in figures 5*a* and 5*b*, respectively. DCM = deep chlorophyll maximum; SSL = subsurface layer; SL = surface layer.

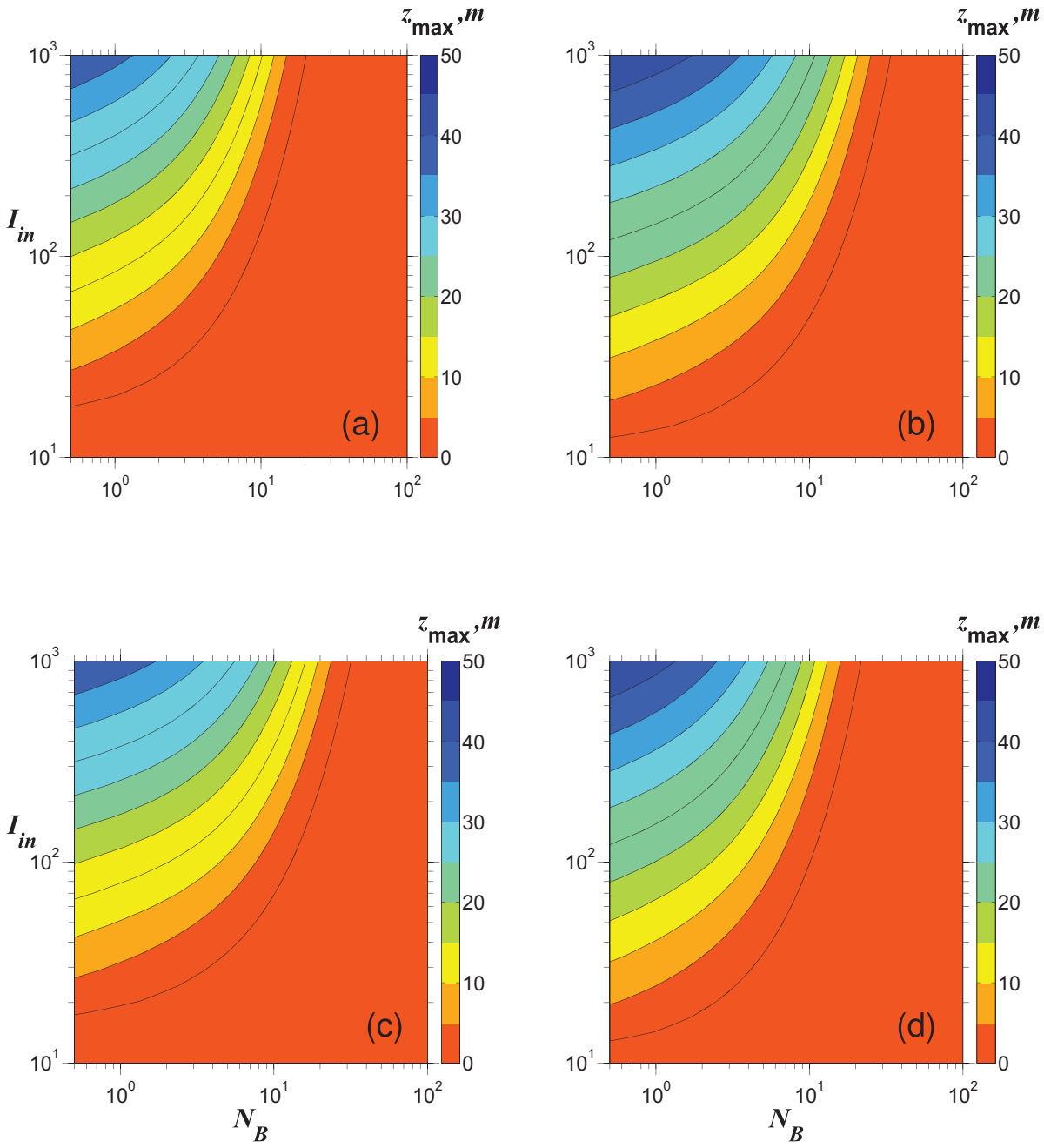

Figure B2: Depth of the production maximum z_{max} of a single species in the (N_B, I_{in}) plane for monocultures of species 1 (*a*), species 2 (*b*), species 1′ (*c*), and species 2′ (*d*).

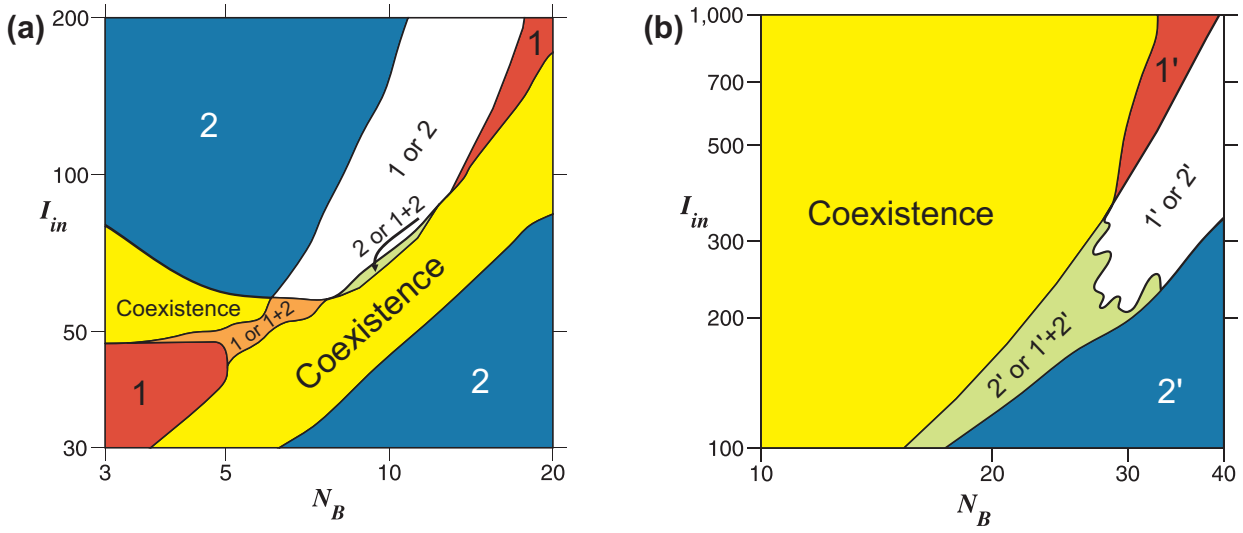

Figure B3: Outcomes of competition between species 1 and 2 (*a*) and between species 1′ and 2′ (*b*), in the ranges of resource supplies marked by green boxes in figures 5*a* and 5*b*, respectively. In addition to the regimes of single-species dominance (red and blue areas) and coexistence (yellow), we observe two kinds of bistability. The first kind of bistability corresponds to a typical scenario where, depending on the initial conditions, either species 1 or species 2 dominates (white areas). The second kind corresponds to a bistability between single-species dominance and two-species coexistence (species 1 dominates in orange areas, species 2 in green areas). In this case, only one (dominant) species can invade in the presence of its competitor (nondominant species). But its invasion does not exclude the nondominant species (if established), and the two competitors can coexist. In contrast, the nondominant species cannot invade the monoculture of the dominant species. In this second bistability regime, the invasibility criterion fails, because it predicts that the dominant competitor should win. It occurs at the boundaries between regimes of coexistence and bistability regimes of the first kind.

Dependence on the Model Parameters

In this section, we explore the impact of the model parameters on the IT slopes (see figs. B4, B5). In each experiment we vary only a single parameter, while the others take their default values (table A1, with species 2 as the resident). In general, variations in the parameters preserve the characteristic shape of the curve $\gamma(N_B)$, with three easily distinguishable intervals: DCM, where γ decays with N_B; SSL, where γ starts to rise and reaches a local maximum at intermediate nutrient concentrations; and SL, where γ drops to 0. However, as we show below, the influence of these variations on the invasibility conditions is often counterintuitive.

Influence of Species Parameters

α, k

Figure B4*a*, B4*b* shows the dependence of the IT slope on the amount of nutrients consumed per resident's cell (α) and light attenuation per cell (k). These coefficients can be conditionally called the consumption rates, because they define the impact of a growing population on the resource levels and therefore play a role similar to that of the consumption rates in resource-ratio theory (Tilman 1980). As shown in figure B4*a*, B4*b*, these rates affect the IT slope differently under oligotrophic and eutrophic conditions. In the range of low N_B, where we observe a DCM or SSL, the value of γ increases with k and decreases with α. Thus, the necessary condition of coexistence, $\gamma_1 < \gamma_2$, will be satisfied if species 1 has a lower k/α ratio than species 2. In contrast, in the range of high N_B, the point where γ drops to 0 (corresponding to a transition into the SL) shifts to the left with increasing k/α. Therefore, in the SL the condition for coexistence can be satisfied only if species 1 has a higher k/α ratio than species 2.

As a consequence, the interior layers (DCM and SSL) and the surface layer (SL) favor the coexistence of two distinct phytoplankton groups. While for coexistence in the interior layers each species should consume mostly its least limiting resource (see also Ryabov and Blasius 2011), in the surface layer each competitor should mostly reduce its most limiting resource. The first rule is diametrically opposed to, and the last rule coincides with, that for uniform systems.

H_I, H_N

The half-saturation constants are important species parameters in our model because they drive the species critical resource values (eq. [5]). As shown in figure B4*c*, decreasing H_I (i.e., light requirements) of the resident favor good nutrient competitors under mesotrophic and eutrophic nutrient conditions (when an SSL or SL occurs). At the same time, decreasing H_N (i.e., nutrient requirements) of the resident favor species with low light requirements in the DCM regime (fig. B4*d*). Thus, simply a difference in resource requirements leads to a shallower IT slope for a good nutrient competitor and a steeper IT slope for a good light competitor, thereby favoring their coexistence (see fig. 1*d*). This effect can compensate for or amplify the effect of consumption rates. In particular, because of this effect the areas of coexistence in figures 5*a* and 5*b* are greater than the areas of bistability.

Influence of Environmental Parameters

Figure B5 shows the dependence of the IT slope on the main environmental parameters: the incident light intensity (I_{in}), water column depth (Z_B), background turbidity (K_{bg}), and turbulent diffusivity (D).

I_{in}

Increasing the incident light intensity, I_{in}, favors good nutrient competitors under mesotrophic and eutrophic conditions. At the same time, under oligotrophic conditions it expands the niche for good light competitors (fig. B5*a*). The latter occurs because increasing I_{in} leads to higher density of the biomass maximum and increases γ until $k\overline{P} < K_{bg}$ (see eq. [B7]). Note also that the subsurface-layer effect (i.e., the local maximum of the curve $\gamma(N_B)$) disappears with decreasing I_{in}.

Z_B

A decrease in the depth of the water column, Z_B, rescales the function $\gamma(N_B)$ along the horizontal axis but almost does not affect its vertical extent (fig. B5*b*). Thus, in a shallow water column the system should exhibit behavior similar to that in a deep water column, but scaled to a narrower range of nutrient supplies.

K_{bg}

There is a common opinion that an increase of water turbidity should increase competition for light and therefore favor good light competitors. As shown in figure B5*c*, this is true only under eutrophic conditions, because the point where $\gamma(N_B)$ drops to 0 then shifts to the left. If, however, the biomass maximum is located in the deep layers, the effect is just the opposite: increasing the background turbidity expands the niche for good nutrient competitors (see Ryabov 2012 for details). Note also that the subsurface-layer effect disappears in turbid water.

D

Another common opinion states that a higher level of turbulent diffusivity, D, should favor good light competitors because it increases the nutrient transport. As shown in figure B5*d*, this is true only under eutrophic conditions (SL), because this relaxes the nutrient limitation. However, under oligotrophic and mesotrophic conditions (DCM and SSL), this gives rise to just the opposite effect: an increase in the niche for good nutrient competitors (see Ryabov 2012 for details). Note also the similarity between the effects of D and k of the resident species on the invasibility conditions (fig. B4*a*).

Lake Tanganyika

The vertical composition of phytoplankton was screened in Lake Tanganyika from 2002 through 2006 at two stations, Mpulungu and Kigoma (Descy et al. 2005, 2010). During so-called wet season (October–April), this lake is characterized by high stability of the water column. To exclude the relaxation processes at the onset of the wet season, we selected the data from October 15 to April 30.

During this time, Lake Tanganyika was dominated by chlorophytes and cyanobacteria, with a small percentage of other phytoplankton taxa. Chlorophytes were of the coccal type, represented by unicells, colonies, and coenobia. Cyanobacteria were represented by two types: T1 (mainly *Synechococcus*) and T2 (filamentous forms, which can adjust their buoyancy). T1 dominated off Mpulungu, while both types were almost equally represented off Kigoma. For the sake of simplicity, we aggregated these two types into one group of cyanobacteria; similar patterns can be obtained considering competition between chlorophytes and T1 only. The other phytoplankton groups (e.g., diatoms) typically contributed less than 10% to the total biomass; with their inclusion, the pattern shown in figure B6 changes only slightly.

To find the phytoplankton biomass and average depth, we interpolated the vertical phytoplankton profiles with 1-m resolution, and the biomass of each group was found as

$$B_i = \int_0^{Z_B} P_i(z)dz,$$

where Z_B is the water column depth and $P_i(z)$ are the densities of cyanobacteria and chlorophytes (μg chlorophyll-a L^{-1}). The percentage of cyanobacteria was found as $B_{cyano}/(B_{cyano} + B_{chlorophytes})$. The location of the bulk of the biomass was calculated as the average depth of the biomass,

$$\langle z \rangle = \frac{\int_0^{Z_B} \sum_i z P_i dz}{\int_0^{Z_B} \sum_i P_i dz}.$$

A comparison of species compositions obtained at Mpulungu and Kigoma is shown in figure B6. The depth and species composition at Kigoma have less variability, and we observed only a part of the whole pattern that can be seen at Mpulungu. This is likely because the environmental conditions are more stable in the Kigoma region than in Mpulungu.

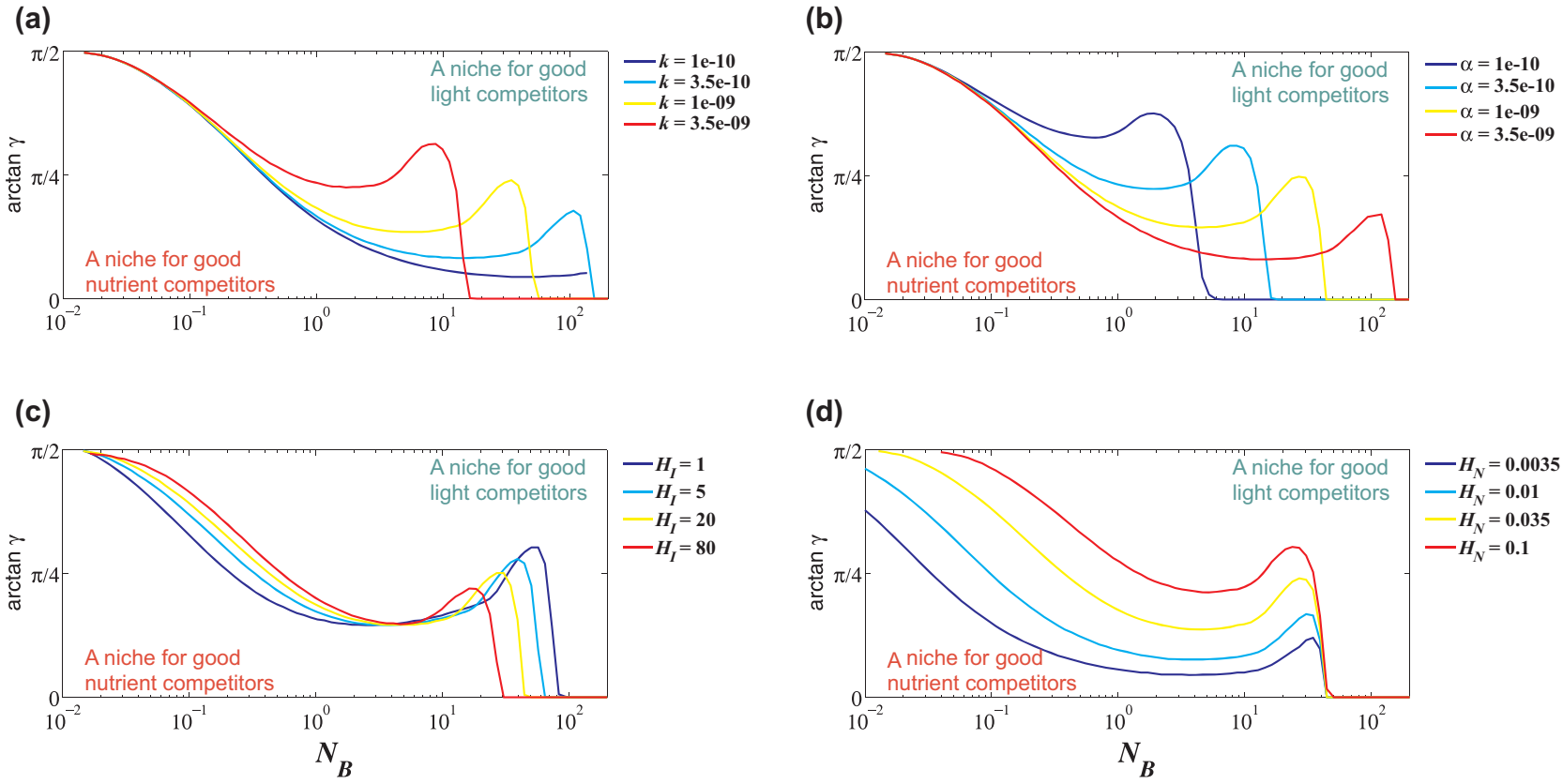

Figure B4: Influence of species traits on invasibility. Slope of the invasion threshold, arctan γ, in dependence of the nutrient supply N_B for different parameters of the resident species. *a*, *b*, Decreasing the light-attenuation coefficient of the resident, *k*, or increasing the nutrients consumed per resident cell, α, increases the niche for good light competitors in the deep chlorophyll maximum (DCM) and subsurface-layer (SSL) regimes. At the same time, this will also improve conditions for good nutrient competitors in the range of high N_B, because the point where γ drops to 0 (the transition into the surface layer) is shifted to the left. *c*, Decreasing the resident's light requirements (lowering H_I) decreases the niche for good nutrient competitors in the DCM regime but increases it in the SSL regime. *d*, Decreasing the resident's nutrient requirements (lowering H_N) expands the niche for good light competitors in the DCM and SSL regimes. Parameter values are given in table A1; except for the varying parameter, the resident species is parameterized as species 2.

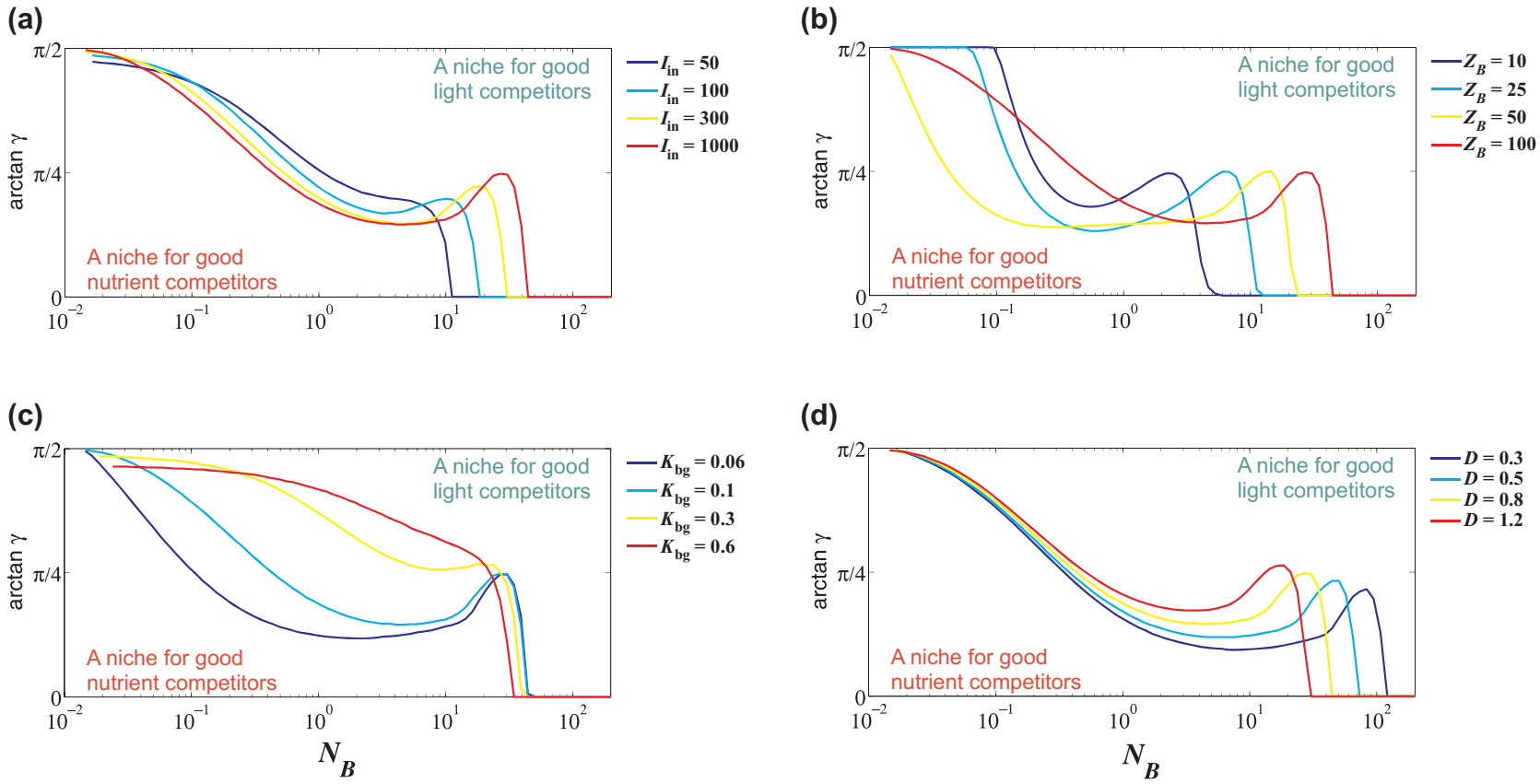

Figure B5: Same as figure B4, but for different environmental parameters. *a*, Increasing the incident light intensity, I_{in}, expands the niche for good light competitors in the deep chlorophyll maximum (DCM) regime but favors the good nutrient competitors in the subsurface-layer (SSL) regime. *b*, The changes of the water column depth, Z_B, rescale the function $\gamma(N_B)$ along the N_B axis but almost do not affect its vertical extent. *c*, Increasing the background turbidity, K_{bg}, increases the niche for good nutrient competitors in the DCM regime and decreases the effect of the SSL. *d*, Increasing the turbulent diffusivity, D, increases the niche for good nutrient competitors in the DCM and SSL regimes.

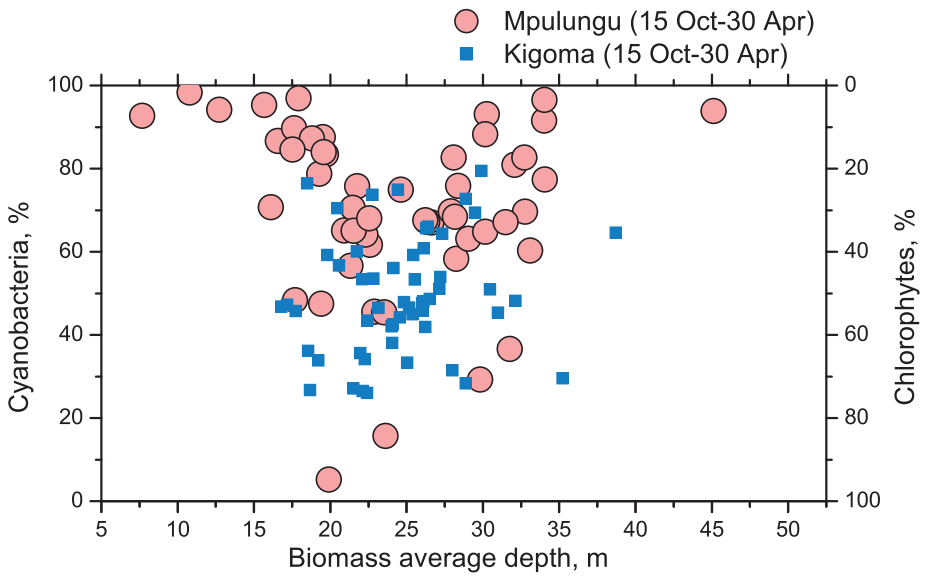

Figure B6: Comparison of the data obtained off Mpulungu (circles) and off Kigoma (squares) during the wet seasons from 2002 to 2006.

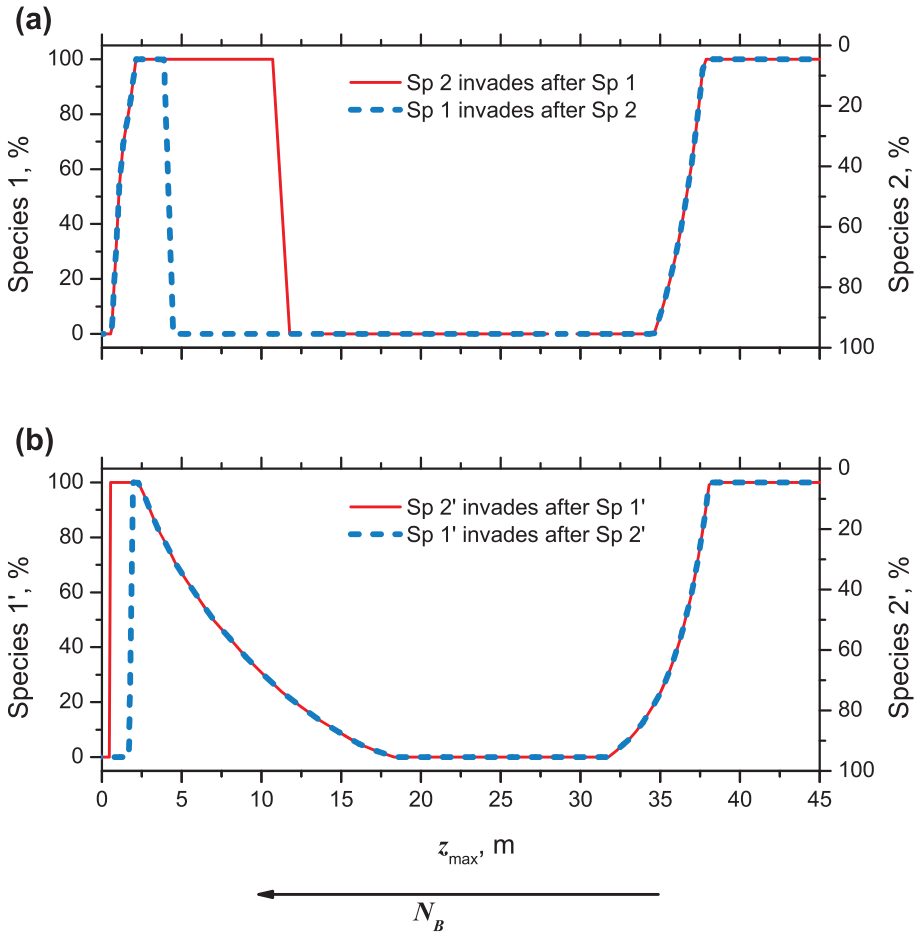

Figure B7: Community composition (percent contribution of species 1 or 2 to the total biomass) as a function of the nutricline, as characterized by z_{max} (calculated along the gradient of N_B shown by the black arrows in fig. 5*a*, 5*b*). The solid lines show the species composition when species 2 invades 2,000 days later than species 1; the dashed lines correspond to the opposite order of invasion. Note that N_B increases from right to left.